



**QUEEN'S
UNIVERSITY
BELFAST**

CaV3.1 T-Type Ca²⁺ Channels Contribute to Myogenic Signalling in Rat Retinal Arterioles

Fernandez, J. A., McGahon, M. K., McGeown, J. G., & Curtis, T. M. (2015). CaV3.1 T-Type Ca²⁺ Channels Contribute to Myogenic Signalling in Rat Retinal Arterioles. *Investigative Ophthalmology and Visual Science*, 56(9), 5125-5132. <https://doi.org/10.1167/iovs.15-17299>

Published in:
Investigative Ophthalmology and Visual Science

Document Version:
Peer reviewed version

Queen's University Belfast - Research Portal:
[Link to publication record in Queen's University Belfast Research Portal](#)

Publisher rights
Copyright 2015 The Association for Research in Vision and Ophthalmology, Inc.

General rights
Copyright for the publications made accessible via the Queen's University Belfast Research Portal is retained by the author(s) and / or other copyright owners and it is a condition of accessing these publications that users recognise and abide by the legal requirements associated with these rights.

Take down policy
The Research Portal is Queen's institutional repository that provides access to Queen's research output. Every effort has been made to ensure that content in the Research Portal does not infringe any person's rights, or applicable UK laws. If you discover content in the Research Portal that you believe breaches copyright or violates any law, please contact openaccess@qub.ac.uk.

**Ca_v3.1 T-Type Ca²⁺ Channels Contribute to Myogenic Signalling in
Rat Retinal Arterioles**

José A. Fernández*, Mary K. McGahon, J. Graham McGeown and Tim M. Curtis *¹

Centre for Experimental Medicine, Queen's University of Belfast

*These authors contributed equally as senior authors.

¹Corresponding author:

Dr Tim Curtis
Centre for Experimental Medicine
Queen's University of Belfast
Institute of Clinical Sciences Block A
Grosvenor Road
Royal Victoria Hospital
Belfast
BT12 6BA
Tel: +44 (0) 2890635027
Email: t.curtis@qub.ac.uk

Word count: 3693

Supported by grants from British Heart Foundation (PG/11/94/29169) and
Biotechnology and Biological Sciences Research Council (BB/I026359/1).

Abstract

Purpose: Although L-type Ca^{2+} channels are known to play a key role in the myogenic reactivity of retinal arterial vessels, the involvement of other types of voltage-gated Ca^{2+} channels in this process remains unknown. In the present study we have investigated the contribution of T-type Ca^{2+} channels to myogenic signalling in arterioles of the rat retinal microcirculation.

Methods: Confocal immunolabelling of wholemount preparations was used to investigate the localisation of $\text{Ca}_v3.1-3$ channels in retinal arteriolar smooth muscle cells. T-type currents and the contribution of T-type channels to myogenic signalling were assessed by whole-cell patch-clamp recording and pressure myography of isolated retinal arteriole segments.

Results: Strong immunolabelling for $\text{Ca}_v3.1$ was observed on the plasma membrane of retinal arteriolar smooth muscle cells. In contrast, no expression of $\text{Ca}_v3.2$ or $\text{Ca}_v3.3$ could be detected in retinal arterioles, although these channels were present on glial cell end-feet surrounding the vessels and retinal ganglion cells, respectively. TTA-A2-sensitive T-type currents were recorded in retinal arteriolar myocytes with biophysical properties distinct from those of the L-type currents present in these cells. Inhibition of T-type channels using TTA-A2 or ML-218 dilated isolated, myogenically active, retinal arterioles.

Conclusions: $\text{Ca}_v3.1$ T-type Ca^{2+} channels are functionally expressed on arteriolar smooth muscle cells of retinal arterioles and play an important role in myogenic signalling in these vessels. The work has important implications concerning our understanding of the mechanisms controlling blood flow autoregulation in the retina and its disruption during ocular disease.

Introduction

It has long been known that alterations in perfusion pressure generate compensatory changes in the diameters of retinal vessels that result in minor or no effects on overall retinal blood flow.¹ A reduced ability of the retina to autoregulate in this manner has been associated with a number of ocular diseases including diabetes, glaucoma and age-related macular degeneration (AMD).²⁻⁶ Vascular autoregulation in the retina is driven by a number of different mechanisms, with both myogenic and metabolic components involved.⁷ The importance of myogenic mechanisms in the regulation of retinal blood flow has been highlighted by several studies performed on isolated retinal arteries and arterioles, showing vasoconstriction or vasodilation in response to either increases or decreases in intravascular pressure, respectively.⁸⁻¹¹

According to the classical view, myogenic responses occur when pressure-induced distension of the vessel wall triggers activation of stretch-activated cation channels on the resident vascular smooth muscle cells, resulting in cell membrane potential depolarisation and increased Ca^{2+} influx through voltage-operated L-type Ca^{2+} channels.¹²⁻¹⁴ This Ca^{2+} influx in turn leads to vascular smooth muscle cell contraction and vessel constriction both directly by increasing the cytosolic Ca^{2+} concentration and indirectly by triggering the release of Ca^{2+} from the sarcoplasmic reticulum via ryanodine (RyR) and inositol trisphosphate receptor channels.¹²⁻¹⁴ We have previously shown that L-type Ca^{2+} channels and RyR receptors play a key role in myogenic signalling in retinal arterioles.^{10,11} These vessels also express voltage-gated $\text{K}_v1.5$ channels^{11,15} and large-conductance Ca^{2+} -activated K^+ channels (BK channels)^{11,16} which act as a brake on the myogenic response mechanism by limiting the degree of pressure-induced depolarisation. Ca^{2+} -activated Cl^- channels have also been found to contribute to the contractile

state of these vessels, although their primary role appears to be in the modulation of agonist-induced tone, rather than myogenic signalling.^{17,18}

Recent studies in other vascular beds have suggested that additional ion channels, such as T-type Ca^{2+} channels, might function as alternative voltage-dependent Ca^{2+} influx pathways that may be involved in the development and maintenance of myogenic tone.^{19,20} Molecular analyses have identified three different isoforms of pore-forming T-type Ca^{2+} channels, namely $\text{Ca}_v3.1$, $\text{Ca}_v3.2$ and $\text{Ca}_v3.3$.^{21,22} Several studies have found some of these to be expressed and functional in resistance vessels,^{23–25} contributing in some cases to myogenic signalling.^{20,23,26–28} T-type Ca^{2+} channels appear to be particularly important in mediating myogenic responses in small arterioles where, despite a loss or decrease in L-type Ca^{2+} currents, development of myogenic tone is still observed.^{26,29,30}

In the present study, we have investigated for the first time the possible involvement of T-type Ca^{2+} channels in the myogenic reactivity of rat retinal arterioles. Using immunohistochemistry, we show that although all three T-type Ca^{2+} channel isoforms are expressed in retinal tissue, only $\text{Ca}_v3.1$ localises to retinal arteriolar smooth muscle cells. We also demonstrate the functional expression of T-type Ca^{2+} channels on the plasma membrane of these cells and characterise their biophysical and pharmacological properties. Finally, we show that two structurally distinct T-type Ca^{2+} channel blockers dilate isolated pressurised retinal arterioles under conditions of steady state myogenic tone, suggesting that these channels make a significant contribution to myogenic signalling in these vessels. These findings have important implications for our understanding of the mechanisms controlling retinal blood flow in both health and disease.

Methods

Animal use conformed to the standards in the ARVO Statement for the Use of Animals in Ophthalmic and Vision Research. Male Sprague-Dawley rats (8–12 weeks of age; 200–250g; Harlan, Bicester, UK) were euthanized with CO₂ in accordance with guidelines contained within the UK Animals (Scientific Procedures) Act of 1986 and approved by the Queen's University of Belfast Animal Welfare and Ethical Review Body.

Immunohistochemistry

Immunohistochemistry was carried out on retinal arterioles embedded within retinal flatmount preparations as described previously.¹⁶ Briefly, freshly enucleated eyes were placed in low Ca²⁺ Hanks solution (see Drugs and Solutions) and hemisected along the ora serrata. The vitreous was removed and the posterior eyecup fixed with 4% paraformaldehyde (PFA) for 20 minutes and then washed extensively in phosphate buffered saline (PBS) for 1 hour. Retinas were subsequently detached and incubated overnight in permeabilisation and blocking buffer (0.05% Triton X-100 and 1% donkey serum in PBS; Sigma, Poole, Dorset, UK, and Millipore, Watford, UK) and then incubated in primary antibody in permeabilisation and blocking buffer for 3 days at 4°C. Primary antibodies, selected on the basis of their specificity towards rat Ca_v3.1–3 channels (Table 1) were employed in conjunction with mouse anti- α -smooth muscle actin (α SMA) antibody (1:200; Sigma) to positively identify vascular smooth muscle cells or isolectin B4 (1:50; Sigma)³¹ to label vascular plasma membranes. Following extensive washing (4 hours at 21°C in PBS), donkey anti-rabbit IgG labelled with Alexa-488 (Life Technologies, Paisley UK; 1:200 in permeabilisation and blocking buffer) or Streptavidin 568 (Life Technologies; 1:500)

were used for Ca_v3.1–3 channel and vascular cell membrane detection, respectively (incubated 4°C overnight). The αSMA primary antibody was conjugated to Cy3, so no secondary antibody was required. Nuclei were labelled with the far-red nuclear stain TOPRO3 (1:1000; Life Technologies; pseudo-coloured blue in relevant images). The immunohistochemistry for each of the Ca_v3.1–3 isoforms was repeated using 4–8 retinas from at least 4 different animals. Secondary only controls and blocking peptide experiments for Ca_v3.1 (10 μg/ml blocking peptide) were also performed. Images were acquired using a Leica SP5 confocal laser scanning microscope (Leica Geosystems; Heerbrugg, Switzerland; HCX PL APO 63x OIL immersion lens) equipped with Argon, HeNe 543 and HeNe 633 lasers. Images were captured in sequential scanning mode with emission wavelengths appropriate for the fluorophores used to reduce overlap (bleed-through) of signals.

Isolated Arteriolar Preparation

For electrophysiology and pressure myography experiments, isolated retinal arteriole segments were used.³² Retinas were dissected from freshly enucleated eyes, placed in low Ca²⁺ Hanks' solution and mechanically triturated using a fire-polished Pasteur pipette. Homogenate was pipetted into a glass-bottomed recording bath mounted on an inverted microscope (Eclipse TE300; Nikon, Tokyo, Japan) and isolated retinal arterioles (length, 100–4000 μm; outer diameter, 15–40 μm) anchored down with tungsten wire slips as described previously.¹⁶ Arterioles were continuously superfused with normal Hanks' solution at 37°C during experimentation. Drugs were delivered via a gravity-fed multi-channel perfusion manifold connected to a single outlet needle that was positioned adjacent to the vessel of interest.

Electrophysiological Recordings

Whole-cell membrane currents were recorded from individual arteriolar smooth muscle cells still embedded within their parental arterioles using the perforated patch-clamp technique.³³ Prior to patching, the vessels were superfused with collagenase 1A (0.1 mg/ml, 10 minutes; Sigma), protease type XIV (0.01 mg/ml, 10 minutes; Sigma) and DNase I (0.02 mg/ml, 5 minutes; Millipore) in low Ca^{2+} Hanks' solution to remove surface basal lamina, electrically uncouple endothelial cells from overlying arteriolar smooth muscle cells and individual smooth muscle cells from one another, and to remove extraneous DNA.^{15,33} Once the whole-cell perforated configuration was acquired, the external Hanks' solution was switched to divalent free solution (see Drugs and Solutions) to enhance the magnitude of currents flowing through voltage-gated Ca^{2+} channels and to prevent interference by Ca^{2+} -activated Cl^- currents.^{34,35} Pipettes pulled from filamented borosilicate glass capillaries (1.5 mm o.d. w 1.17 mm i.d., Harvard Instruments, Kent, UK) were fire polished to resistances of 1-2 M Ω . Membrane currents were recorded using an Axopatch 200B patch-clamp amplifier (Molecular Devices, CA, USA), low pass filtered at 0.5 kHz and sampled at 2 kHz. Voltage step protocols were applied using pClamp (version 10.2; Molecular Devices) via a Digidata 1440A interface (Molecular Devices). Leak currents were subtracted off-line from the active currents using the response to a hyperpolarizing step from a holding potential of -80 mV to -90 mV as the correction signal. Calculation and plotting of difference curves, off-line leak subtraction and fitting of exponentials was performed using purpose-written software in R.³⁶

Arteriolar Myography

The involvement of T-type Ca^{2+} channels in the generation of arteriolar myogenic tone was assessed using pressure myography as previously described.¹⁶ A tungsten

170 wire slip was laid on the arteriole, anchoring and occluding one end. The vessel was
171 then superfused with Ca^{2+} -free Hanks' solution. The open end was cannulated using
172 a glass micropipette (1.5mm o.d., 0.86 i.d. tapered to a tip diameter of 2–5 μm) filled
173 with Ca^{2+} -free Hanks' solution, using a patch-clamp electrode holder and
174 micromanipulator (Molecular Devices). Once the pipette tip had been appropriately
175 positioned, the pipette was advanced so as to wedge it tightly into the lumen of the
176 vessel. To ensure there was no significant flow through the vessel or leakage of fluid
177 around the cannulation site, a small air bubble was introduced into the tubing
178 connecting the cannulating pipette to the manometer. Only vessels where this
179 bubble remained relatively static following pressurisation were used for
180 experimentation. Following introduction of the pipette, the vessel was superfused
181 with normal Hanks' solution for 10–15 minutes, allowing the pipette to seal to the
182 inner vessel wall. Vessels were then pressurised to 40 mmHg and left at that
183 pressure until stable myogenic tone had fully developed (usually ~10 minutes).
184 Intraluminal pressure was regulated by using a manometer connected to the
185 cannulating micropipette (Riester "Big Ben" pressure manometer; Riester,
186 Jungingen, Germany). The maximum passive diameter of the vessels was
187 determined by application of the myosin light chain kinase inhibitor, wortmannin (10
188 μM),^{37,38} in the presence of Ca^{2+} -free Hanks' solution at the end of the experiment.
189 This value was used to normalise vessel diameter data across individual arterioles.
190 Vessels were viewed under a 20x, NA 0.4 objective and images (saved as BMP
191 images of 1280x1024 pixels; 8-bit; 1.2MB) captured at a rate of 140 images per
192 minute using a MCN-B013-U USB camera (Mightex, Pleasanton, CA, USA).
193 Acquisition was carried out using custom software implemented in Delphi.¹⁶ The

measurement of vessel diameters and tracking of diameter changes was performed using the MyoTracker software package.³⁹

Drugs and Solutions

The composition of the solutions used was as follows (in mM): Normal Hanks' solution - 140, NaCl; 6, KCl; 5, D-glucose; 2, CaCl₂; 1.3, MgCl₂; 10, HEPES; pH set to 7.4 with NaOH; Divalent free solution - 120, NaCl; 5, KCl; 5, D-glucose; 10, HEPES; 5, EGTA; 20, Tetraethylammonium Chloride (TEA); K⁺-based internal pipette solution; 52, KCl; 80, Gluconic acid; 80, KOH; 1, MgCl₂; 0.5, EGTA; 10, HEPES; pH set to 7.2 with KOH. The low Ca²⁺ Hanks' solution was of Hanks' composition, but contained only 0.1 mM Ca²⁺. For the Ca²⁺ free Hanks' solution, Ca²⁺ was omitted. Amphotericin B (final concentration of 0.39 mM) was dissolved in the pipette solutions as the pore-forming agent.

Unless otherwise stated, stock solutions of drugs were initially prepared in DMSO and then diluted to the final concentration. The final bath concentration of DMSO was ≤0.1%. In vehicle control experiments, application of DMSO, at the maximal concentration used in these studies, had no effect on arteriolar diameter (Table 2). Amphotericin B, nimodipine, TEA and EGTA were obtained from Sigma; TTA-A2, ML-218 and wortmannin were purchased from Alomone Labs (Jerusalem, Israel). HEPES was obtained from Melford Laboratories (Ipswich, UK).

Statistical Analysis

Data are presented as the mean ± SEM. Statistical significance was determined by using either paired t-tests (when data conformed to Kolmogorov-Smirnov normality

218 tests) or the Wilcoxon matched-pairs signed rank test for which no assumptions
219 about normality were made. In all comparisons, the 95% level was accepted as
220 statistically significant. Analysis was carried out using Prism 5 for Windows (version
221 5.03; GraphPad Software Inc., La Jolla, CA, USA). In all graphical representations of
222 the data, statistical significance is indicated as follows: NS, $P > 0.05$; $*$ = $P < 0.05$;
223 $**$ = $P < 0.01$; $***$ = $P < 0.001$.

224

Results

Immunolocalisation of T-Type Ca^{2+} Channels in Retinal Arteriolar Smooth Muscle

The expression of the three T-type channel isoforms, $\text{Ca}_v3.1$, $\text{Ca}_v3.2$ and $\text{Ca}_v3.3$, was examined in rat retinal wholemount preparations using immunohistochemistry. Retinal arterioles were identified by positive staining for αSMA with a single monolayer of vascular smooth muscle cells running transversely to the long axis of the vessels (Fig. 1 A). In contrast, venules showed much weaker αSMA staining of pericyte-like mural cells (Fig. 1 B). As shown in Figure 2, strong immunolabelling for $\text{Ca}_v3.1$ proteins was detected on the surface of the retinal arteriolar smooth muscle cells, along with weaker, more diffuse, cytosolic staining (Fig. 2 A). Plasma membrane expression of $\text{Ca}_v3.1$ channels was confirmed by co-localisation with isolectin B4 (Fig. 2 B). In the surrounding retinal neuropile, $\text{Ca}_v3.1$ expression was also localised to retinal ganglion cells (RGCs; Fig. 2 A). Control experiments performed with secondary antibodies only or primary anti- $\text{Ca}_v3.1$ antibodies pre-absorbed with a specific blocking peptide were negative (Fig. 2 C). Expression of $\text{Ca}_v3.2$ was detected in close proximity to the retinal arterioles (Fig. 2 D). However, on closer inspection, it was evident that this expression was limited to the perivascular end-feet of glial cells surrounding the vessels. $\text{Ca}_v3.3$ expression was absent from retinal arterioles, but strong immunolabelling was present in the surrounding retinal neuropile primarily associated with RGCs (Fig. 2 E).

Electrical Characterisation of the T-Type Currents

Whole-cell patch-clamp experiments were conducted to examine the functional expression of T-type Ca^{2+} channels on the plasma membrane of retinal arteriolar smooth muscle cells. Figure 3 shows voltage-dependent inward T-type currents sensitive to external application of the selective T-type Ca^{2+} channel inhibitor, TTA-A2 (1 μM ; Fig. 3 A, left panel),^{40,41} and L-type currents sensitive to nimodipine (1 μM ; Fig. 3 A, right panel)¹⁰. Representative and average current-voltage (I - V) relationships for both TTA-A2- and nimodipine-sensitive currents are also shown (Fig. 3 B, left and right panels, respectively). As can be seen, the TTA-A2-sensitive I - V curve activates at a more negative membrane potential than the nimodipine-sensitive current (-70 mV for the T-type current compared to -50 mV for the L-type current; Fig. 3 B). This is also the case for the peak currents, with T-type current peaking at around -30 to -20 mV, compared to -10 to 0 mV for the L-type current (Fig. 3 B). These currents also displayed significant differences in their rates of activation and inactivation, with the T-type currents having a faster rate of both activation (T_{ac} 4.3 ± 0.7 versus 8.2 ± 1.3 ms) and inactivation (T_{inac} 18.2 ± 1 versus 24.1 ± 1.5 ms) compared with the L-type currents ($P < 0.01$ in both cases, $n=8$; Fig. 3 C and D). Thus, these results confirm that T-type Ca^{2+} channels are functionally expressed in retinal arteriolar smooth muscle cells, and in the final experiments, analyses were performed to examine their possible role in the myogenic reactivity of retinal arterioles.

Blocking T-Type Ca^{2+} Channels Causes Dilation of Pressurised Retinal Arterioles

To investigate the possible role of T-type channels in myogenic signalling, we carried out pressure myography experiments on isolated retinal arterioles. Vessels were cannulated and pressurised to 40 mmHg until myogenic tone had fully developed and stabilised. Arterioles were then exposed to TTA-A2 (1 μM) or another selective T-type Ca^{2+} channel blocker, ML-218 (1 μM),⁴² and changes in vessel diameter recorded. At the end of the experiment, wortmannin (10 μM), was applied in Ca^{2+} -free Hanks' solution in order to obtain the maximal passive diameter of the vessels. Both TTA-A2 and ML-218 caused a significant dilation of myogenically active rat retinal arterioles by ~50% of the maximal passive diameter ($P < 0.001$, Wilcoxon matched-pairs signed rank test; Fig. 4 A and B, Table 2). These findings are consistent with the view that T-type Ca^{2+} channels contribute to the generation of myogenic tone in these vessels.

Discussion

This study shows for the first time that the T-type Ca^{2+} channel isoform, $\text{Ca}_v3.1$, is functionally expressed in vascular smooth muscle cells of rat retinal arterioles and plays an important role in myogenic signalling in these vessels. Although we found no evidence for expression of $\text{Ca}_v3.2$ or $\text{Ca}_v3.3$ channels in these vessels, these isoforms were identified in glial cell end-feet surrounding the vessels ($\text{Ca}_v3.2$; Fig. 2 D) and RGCs ($\text{Ca}_v3.3$; Fig. 2 E). Our results are consistent with previous studies reporting $\text{Ca}_v3.1$ expression in vascular smooth muscle cells of other vascular beds, including those of the renal, skeletal muscle, mesenteric, brain and pulmonary circulations.^{23,24,27,30,43–45} Although expression of $\text{Ca}_v3.3$ has not been widely reported in vascular smooth muscle cells, $\text{Ca}_v3.2$ has been detected in cerebral and pulmonary artery myocytes.^{20,45} Recent work has established that Ca^{2+} influx through vascular smooth muscle $\text{Ca}_v3.2$ channels is principally involved in mediating vasodilatory responses via activation of RyR-dependent Ca^{2+} sparks and BK channels.²⁸ It would appear unlikely, however, that such a mechanism is active in retinal arterioles, given that $\text{Ca}_v3.2$ channels could not be detected in these vessels.

Consistent with the presence of $\text{Ca}_v3.1$ channels on the plasma membrane of retinal arteriolar myocytes, we identified T-type currents with pharmacological and kinetic features similar to those produced by $\text{Ca}_v3.1$ subunits in other systems (Fig. 3).^{21,46} These currents were different from the L-type voltage-dependent Ca^{2+} currents in these cells in that they were activated at lower membrane potentials and had faster kinetic rates of activation and inactivation (Fig. 3). Similar kinetic rates have been reported for T-type channels in other vascular tissues.^{21,28,47} Some studies carried out on mesenteric and cerebral arteries, however, have reported an unexpected depolarising shift in the activation and inactivation profiles of these

channels compared to traditional T-type channels, leading to the suggestion that in vascular myocytes the T-type channels may be formed from splice variants.⁴⁸ In our study, however, we could detect two clearly distinguishable peaks in the *I-V* curves for T-type and L-type currents, closer to traditional T-type values, and the peak *I-V* values shown here (–30 to –20 mV) closely match those reported for T-type currents in other cells, including neurons, cardiomyocytes and coronary and aortic vascular smooth muscle cells.²¹

Although L-type Ca^{2+} channels are generally believed to play a central role in the development of myogenic tone,¹³ it has been noted in several studies that L-type Ca^{2+} channel inhibition does not completely abolish the myogenic response.^{19,20,49–51} In the present study, we have demonstrated that two different T-type blockers, TTA-A2 and ML-218, are capable of partially inhibiting myogenic signalling in isolated rat retinal arterioles (Fig. 4; Table 2). Whilst the absolute changes in vessel diameter that we have recorded following T-type Ca^{2+} channel blockade are relatively small, we have calculated for individual arterioles that these would be expected to decrease vascular resistance in the range of ~3-15% (mean of ~7%; based on $R \propto 1/d^4$).¹⁰ Thus it seems likely that these channels will make at least some contribution to the modulation of retinal blood flow autoregulation *in vivo*. Our data concur with other studies showing that $\text{Ca}_v3.1$ T-type channels play an important role in the development and maintenance of myogenic tone in vessels from several vascular beds. Navarro-Gonzalez et al. (2009), for example, showed that myogenic tone in the rat basilar artery results from Ca^{2+} influx through nifedipine-insensitive voltage-dependent Ca^{2+} channels with characteristics similar to the T-type channel isoform $\text{Ca}_v3.1$.⁴³ Björling et al. (2013), working with mice deficient in the $\text{Ca}_v3.1$ T-type isoform, showed that T-type channels are crucial for myogenic tone in

mesenteric arteries at low arterial pressure (<80 mmHg), but are inactivated at high arterial pressure where L-type Ca^{2+} channels predominate in the myogenic response.^{20,52–54} Since the arterial input pressure in the retina is thought to be ~40 mmHg,^{55,56} and retinal arterioles exhibit myogenic tone between 10 and 70 mmHg,^{9,10,57} these observations would support the view that $\text{Ca}_v3.1$ T-type channels are likely to play an important role in both setting basal vascular tone and in modulating vascular tone in response to changes in systemic blood pressure (i.e. in mediating blood flow autoregulation) in the retinal microcirculation *in vivo*.

In summary, this study is the first to identify $\text{Ca}_v3.1$ T-type currents in vascular smooth muscle cells of retinal arterioles and to characterise their contribution to myogenic signalling in these vessels. The work provides an important foundation for better understanding the mechanisms regulating retinal perfusion in both health and disease. It seems likely, for example, that in addition to contributing to the myogenic reactivity of retinal arterioles, endothelial and glial cell mediators known to modulate retinal vascular tone and blood flow may, at least in part, act by targeting the activity of these channels. In support of this idea, previous studies have shown that vasodilator molecules such as nitric oxide and 5,6 epoxyeicosatrienoic acid are capable of inhibiting T-type Ca^{2+} channel activity,^{58,59} while the vasoconstrictor peptide, endothelin-1, has been shown to enhance currents through these channels.⁶⁰ From a pathophysiological perspective, we currently have only a limited knowledge of the role of T-type Ca^{2+} currents in the development of vascular disease, although $\text{Ca}_v3.1$ channels have been identified as potential therapeutic targets for the prevention of restenosis following angioplasty.⁶¹ Our current work opens up several new avenues for further research. The possibility that alterations in $\text{Ca}_v3.1$ channel expression and activity contribute to the loss of retinal vascular

autoregulation and blood flow disturbances during diseases such as diabetes, glaucoma and AMD now merits further investigation.

References

1. Robinson F, Riva CE, Grunwald JE, Petrig BL, Sinclair SH. Retinal blood flow autoregulation in response to an acute increase in blood pressure. *Invest Ophthalmol Vis Sci.* 1986;27:722–726.
2. Anderson DR. Introductory comments on blood flow autoregulation in the optic nerve head and vascular risk factors in glaucoma. *Surv Ophthalmol.* 1999;43:S5–S9.
3. Evans DW, Harris A, Garrett M, Chung HS, Kagemann L. Glaucoma patients demonstrate faulty autoregulation of ocular blood flow during posture change. *Br J Ophthalmol.* 1999;83:809–813.
4. Ehrlich R, Harris A, Kheradiya NS, Winston DM, Ciulla TA, Wirostko B. Age-related macular degeneration and the aging eye. *Clin Interv Aging.* 2008;3:473–482.
5. Pemp B, Schmetterer L. Ocular blood flow in diabetes and age-related macular degeneration. *Can J Ophthalmol.* 2008;43:295–301.
6. He Z, Vingrys AJ, Armitage JA, Bui BV. The role of blood pressure in glaucoma. *Clin Exp Optom.* 2011;94:133–149.
7. Pournaras CJ, Rungger-Brandle E, Riva CE, Hardarson SH, Stefansson E. Regulation of retinal blood flow in health and disease. *Prog Retin Eye Res.* 2008;27:284–330.
8. Hoste AM, Boels PJ, Brutsaert DL, De Laey JJ. Effect of alpha-1 and beta agonists on contraction of bovine retinal resistance arteries in vitro. *Invest Ophthalmol Vis Sci.* 1989;30:44–50.
9. Delaey C, Van de Voorde J. Pressure-induced myogenic responses in isolated bovine retinal arteries. *Invest Ophthalmol Vis Sci.* 2000;41:1871–1875.
10. Kur J, Bankhead P, Scholfield CN, Curtis TM, McGeown JG. Ca(2+) sparks promote myogenic tone in retinal arterioles. *Br J Pharmacol.* 2013;168:1675–1686.
11. Kur J, McGahon MK, Fernández JA, Scholfield CN, McGeown JG, Curtis TM. Role of ion channels and subcellular Ca²⁺ signaling in arachidonic acid-induced dilation of pressurized retinal arterioles. *Invest Ophthalmol Vis Sci.* 2014;55:2893–2902.
12. Gollasch M, Nelson MT. Voltage-dependent Ca²⁺ channels in arterial smooth muscle cells. *Kidney Blood Press Res.* 1997;20:355–371.
13. Davis MJ, Hill MA. Signaling mechanisms underlying the vascular myogenic response. *Physiol Rev.* 1999;79:387–423.

399 14. Catterall WA. Voltage-gated calcium channels. *Cold Spring Harb Perspect Biol.*
400 2011;3:a003947.

401 15. McGahon MK, Dawicki JM, Arora A, et al. Kv1.5 is a major component
402 underlying the A-type potassium current in retinal arteriolar smooth muscle. *Am J*
403 *Physiol Heart Circ Physiol.* 2007;292:H1001–H1008.

404 16. McGahon MK, Dash DP, Arora A, et al. Diabetes downregulates large-
405 conductance Ca²⁺-activated potassium β 1 channel subunit in retinal arteriolar
406 smooth muscle. *Circ Res.* 2007;100:703–711.

407 17. McGahon MK, Needham MA, Scholfield CN, McGeown JG, Curtis TM. Ca²⁺-
408 activated Cl⁻ current in retinal arteriolar smooth muscle. *Invest Ophthalmol Vis Sci.*
409 2009;50:364–371.

410 18. Needham M, McGahon MK, Bankhead P, et al. The role of K⁺ and Cl⁻ channels
411 in the regulation of retinal arteriolar tone and blood flow. *Invest Ophthalmol Vis Sci.*
412 2014;55:2157–2165.

413 19. Mufti RE, Brett SE, Tran CH, et al. Intravascular pressure augments cerebral
414 arterial constriction by inducing voltage-insensitive Ca²⁺ waves. *J Physiol.*
415 2010;588:3983–4005.

416 20. Abd El-Rahman RR, Harraz OF, Brett SE, et al. Identification of L- and T-type
417 Ca²⁺ channels in rat cerebral arteries: role in myogenic tone development. *Am J*
418 *Physiol Heart Circ Physiol.* 2013;304:H58–H71.

419 21. Perez-Reyes E. Molecular physiology of low-voltage-activated T-type calcium
420 channels. *Physiol Rev.* 2003;83:117–161.

421 22. Perez-Reyes E. Molecular characterization of T-type calcium channels. *Cell*
422 *Calcium.* 2006;40:89–96.

423 23. Hansen PB, Jensen BL, Andreassen D, Skøtt O. Differential expression of T- and
424 L-type voltage-dependent calcium channels in renal resistance vessels. *Circ Res.*
425 2001;89:630–638.

426 24. Jensen LJ, Salomonsson M, Jensen BL, Holte-Rathlou NH. Depolarization-
427 induced calcium influx in rat mesenteric small arterioles is mediated exclusively via
428 mibefradil-sensitive calcium channels. *Br J Pharmacol.* 2004;142:709–718.

429 25. Hayashi K, Wakino S, Homma K, Sugano N, Saruta T. Pathophysiological
430 significance of T-type Ca²⁺ channels: role of T-type Ca²⁺ channels in renal
431 microcirculation. *J Pharmacol Sci.* 2005;99:221–227.

432 26. Gustafsson F, Andreassen D, Salomonsson M, Jensen BL, Holstein-Rathlou N.
433 Conducted vasoconstriction in rat mesenteric arterioles: role for dihydropyridine-
434 insensitive Ca(2+) channels. *Am J Physiol Heart Circ Physiol.* 2001;280:H582–H590.

435 27. VanBavel E, Sorop O, Andreassen D, Pfaffendorf M, Jensen BL. Role of T-type
436 calcium channels in myogenic tone of skeletal muscle resistance arteries. *Am J*
437 *Physiol Heart Circ Physiol.* 2002;283:H2239–H2243.

438 28. Harraz OF, Abd El-Rahman RR, Bigdely-Shamloo K, et al. Ca(V)_{3.2} channels
439 and the induction of negative feedback in cerebral arteries. *Circ Res*. 2014;115:650–
440 661.

441 29. Morita H, Cousins H, Onoue H, Ito Y, Inoue R. Predominant distribution of
442 nifedipine-insensitive, high voltage-activated Ca²⁺ channels in the terminal
443 mesenteric artery of guinea pig. *Circ Res*. 1999;85:596–605.

444 30. Braunstein TH, Inoue R, Cribbs L, et al. The role of L- and T-type calcium
445 channels in local and remote calcium responses in rat mesenteric terminal arterioles.
446 *J Vasc Res*. 2009;46:138–151.

447 31. Peppiatt C, Lahne M, Howarth C, Attwell D, Mobbs P. Confocal imaging of
448 isolectin B4 labelling as a tool for studying neuronal-capillary interactions in living
449 cerebellar slices and retina from rats. *Proceedings of The Physiological Society: J*
450 *Physiol*. 2004;555P,PC21.

451 32. Scholfield CN, Curtis TM. Heterogeneity in cytosolic calcium regulation among
452 different microvascular smooth muscle cells in rat retina. *Microvasc Res*.
453 2000;59:233–242.

454 33. McGahon MK, Dawicki JM, Scholfield CN, McGeown JG, Curtis TM. A-type
455 potassium current in retinal arteriolar smooth muscle cells. *Invest Ophthalmol Vis*
456 *Sci*. 2005;46:3281–3287.

457 34. McDonald TF, Pelzer S, Trautwein W, Pelzer DJ. Regulation and modulation of
458 calcium channels in cardiac, skeletal, and smooth muscle cells. *Physiol Rev*.
459 1994;74:365–507.

460 35. Large WA, Wang Q. Characteristics and physiological role of Ca²⁺-activated Cl-
461 conductance in smooth muscle. *Am J Physiol*. 1996;271:C435–C454.

462 36. R Development Core Team. 2014. R: A language and environment for statistical
463 computing. R Foundation for Statistical Computing, Vienna, Austria. URL
464 <http://www.R-project.org/>

465 37. Nakanishi S, Kakita S, Takahashi I, et al. Wortmannin, a microbial product
466 inhibitor of myosin light chain kinase. *J Biol Chem*. 1992;267:2157–2163.

467 38. Burdyga TV, Wray S. The effect of inhibition of myosin light chain kinase by
468 Wortmannin on intracellular [Ca²⁺], electrical activity and force in phasic smooth
469 muscle. *Pflugers Arch*. 1998;436:801–803.

470 39. Fernández JA, Bankhead P, Zhou H, McGeown JG, Curtis TM. Automated
471 detection and measurement of isolated retinal arterioles by a combination of edge
472 enhancement and cost analysis. *PLoS One*. 2014;9:e91791.

473 40. Uebele VN, Gotter AL, Nuss CE, et al. Antagonism of T-type calcium channels
474 inhibits high-fat diet-induced weight gain in mice. *J Clin Invest*. 2009;119:1659–1667.

475 41. Kraus RL, Li Y, Grogan Y, et al. In vitro characterization of T-type calcium
476 channel antagonist TTA-A2 and in vivo effects on arousal in mice. *J Pharmacol Exp*
477 *Ther*. 2010;335:409–417.

478 42. Xiang Z, Thompson AD, Brogan JT, et al. The discovery and characterization of
479 ML218: a novel, centrally active T-type calcium channel inhibitor with robust effects
480 in STN neurons and in a rodent model of Parkinson's disease. *ACS Chem Neurosci*.
481 2011;2:730–742.

482 43. Navarro-Gonzalez MF, Grayson TH, Meaney KR, Cribbs LL, Hill CE. Non-L-Type
483 voltage-dependent calcium channels control vascular tone of the rat basilar artery.
484 *Clin Exp Pharmacol Physiol*. 2009;36:55–66.

485 44. Pluteanu F, Cribbs LL. Regulation and function of Cav3.1 T-type calcium
486 channels in IGF-I-stimulated pulmonary artery smooth muscle cells. *Am J Physiol*
487 *Cell Physiol*. 2011;300:C517–C525.

488 45. Chevalier M, Gilbert G, Roux E, et al. T-type calcium channels are involved in
489 hypoxic pulmonary hypertension. *Cardiovasc Res*. 2014;103:597–606.

490 46. Klöckner U, Lee JH, Cribbs LL, et al. Comparison of the Ca²⁺ currents induced
491 by expression of three cloned alpha1 subunits, alpha1G, alpha1H and alpha1I, of
492 low-voltage-activated T-type Ca²⁺ channels. *Eur J Neurosci*. 1999;11:4171–4178.

493 47. Kuo IY, Ellis A, Seymour VA, Sandow SL, Hill CE. Dihydropyridine-insensitive
494 calcium currents contribute to function of small cerebral arteries. *J Cereb Blood Flow*
495 *Metab*. 2010;30:1226–1239.

496 48. Kuo IY, Howitt L, Sandow SL, McFarlane A, Hansen PB, Hill CE. Role of T-type
497 channels in vasomotor function: team player or chameleon? *Pflugers Arch*.
498 2014;466:767–779.

499 49. Beltrame JF, Turner SP, Leslie SL, Solomon P, Freedman SB, Horowitz JD. The
500 angiographic and clinical benefits of mibefradil in the coronary slow flow
501 phenomenon. *J Am Coll Cardiol*. 2004;44:57–62.

502 50. Oshima T, Ozono R, Yano Y, et al. Beneficial effect of T-type calcium channel
503 blockers on endothelial function in patients with essential hypertension. *Hypertens*
504 *Res*. 2005;28:889–894.

505 51. Velat GJ, Kimball MM, Mocco JD, Hoh BL. Vasospasm after aneurysmal
506 subarachnoid hemorrhage: review of randomized controlled trials and meta-analyses
507 in the literature. *World Neurosurg*. 2011;76:446–454.

508 52. Björling K, Morita H, Olsen MF, et al. Myogenic tone is impaired at low arterial
509 pressure in mice deficient in the low-voltage-activated Ca_v 3.1 T-type Ca(2+)
510 channel. *Acta Physiol (Oxf)*. 2013;207:709–720.

511 53. Kuo IY, Wolfle SE, Hill CE. T-type calcium channels and vascular function: the
512 new kid on the block? *J Physiol*. 2011;589:783–795.

513 54. Hansen PB. Functional importance of T-type voltage-gated calcium channels in
514 the cardiovascular and renal system: news from the world of knockout mice. *Am J*
515 *Physiol Regul Integr Comp Physiol*. 2015;308:R227–R237.

516 55. Takahashi T, Nagaoka T, Yanagida H, et al. A mathematical model for the
517 distribution of hemodynamic parameters in the human retinal microvascular network.
518 *J Biorheol*. 2009;23:77–86.

56. Arciero J, Harris A, Siesky B, et al. Theoretical Analysis of Vascular Regulatory Mechanisms Contributing to Retinal Blood Flow Autoregulation. *Invest Ophthalmol Vis Sci.* 2013;54:5584–5593.
57. Jeppesen P, Aalkjaer C, Bek T. Myogenic response in isolated porcine retinal arterioles. *Curr Eye Res.* 2003;27:217–222.
58. Harraz OF, Brett SE, Welsh DG. Nitric oxide suppresses vascular voltage-gated T-type Ca²⁺ channels through cGMP/PKG signaling. *Am J Physiol Heart Circ Physiol.* 2014;306:H279–H285.
59. Cazade M, Bidaud I, Hansen PB, Lory P, Chemin J. 5,6-EET potently inhibits T-type calcium channels: implication in the regulation of the vascular tone. *Pflugers Arch.* 2014;466:1759–68.
60. Park JY, Kang HW, Moon HJ, et al. Activation of protein kinase C augments T-type Ca²⁺ channel activity without changing channel surface density. *J Physiol.* 2006;577:513–23.
61. Tzeng BH, Chen YH, Huang CH, Lin SS, Lee KR, Chen CC. The Ca(v)3.1 T-type calcium channel is required for neointimal formation in response to vascular injury in mice. *Cardiovasc Res.* 2012;96:533-542.

Figure legends

Figure 1. (A) Arteriole and (B) venule within a retinal wholemount preparation immunolabelled for α -SMA (red channel). Nuclei were labelled with the far-red nuclear stain TOPRO3 (pseudo-coloured blue).

Figure 2. Distribution patterns of $\text{Ca}_v3.1-3$ T-type channel isoforms in retinal arterioles and the surrounding retinal parenchyma (A) Top panel, rat retinal wholemount preparation immunolabelled for $\text{Ca}_v3.1$ (green channel), α SMA (red channel) and cell nuclei (blue channel; TOPRO3). Bottom panel, $\text{Ca}_v3.1$ staining segmented from the same image. (B) Individual and merged images showing $\text{Ca}_v3.1$ (green channel) co-localisation with the plasma membrane marker, isolectin B4 (red channel), in retinal arteriolar myocytes. (C) Top panel, secondary only control image. Bottom panel, blocking peptide experiment for the anti- $\text{Ca}_v3.1$ primary antibody. (D, E) Equivalent immunolabelling to that shown in A, but for $\text{Ca}_v3.2$ and $\text{Ca}_v3.3$ isoforms, respectively.

Figure 3. (A) TTA-A2-sensitive T-type currents (left panel) and nimodipine-sensitive L-type currents (right panel) elicited in response to voltage steps from -80 to +40mV in 10 mV increments from a holding potential of -80 mV. Current traces are presented as difference currents. (B) Representative (left) and mean (right) I - V relationships ($n=8$ cells) for the TTA-A2 and nimodipine-sensitive currents. (C) Kinetic rate constants of activation and inactivation for the currents obtained in A. Analysis was carried out on currents obtained at a voltage step to -10 mV (left panel). Dashed boxes indicate both the activation (magnified in the middle panel) and inactivation (magnified in the right panel) of the currents at that voltage.

Activating and inactivating currents were fitted using single exponentials. (D) Mean time constants of activation (left) and inactivation (right) (n=8).

Figure 4. Effects of T-type blockers on the diameter of isolated retinal arterioles under myogenic tone. (A) Representative traces showing the diameters of vessels under steady-state myogenic tone (grey line, actual diameter; black line, smoothed trace showing the moving average of 11 points superimposed on top of the raw diameters) at an intraluminal pressure of 40 mmHg (first 2–3 minutes), dilation of the vessel after application of the T-type blocker (TTA-A2, 1 μ M, left panel; ML-218, 1 μ M, right panel), and subsequent further dilation to the maximal passive diameter after application of wortmannin in Ca^{2+} -free Hanks' solution. (B) Mean arteriole diameters normalised to the maximal diameters following application of DMSO, TTA-A2 or ML-218.

Table 1. Antibodies and dilutions used to investigate $\text{Ca}_v3.1$ –3 protein expression.

Protein	Antibody (Company)	Epitope(species)	Dilution
$\text{Ca}_v3.1$	ACC-021 (Alomone; Jerusalem, Israel)	AA1–22 (rat)	1:200
$\text{Ca}_v3.2$	ACC-025 (Alomone)	AA581–595 (human)	1:200
$\text{Ca}_v3.3$	OSC00263W (Osenses; Keswick, Australia)	AA450-500 (human)	1:200

Table 2. Effects of T-type blockers on the diameters of pressurised retinal arterioles.

Diameters (μm)	After steady-state tone development	In presence of vehicle/inhibitor	Passive diameter	% diameter change
DMSO (n=10)	29.5 \pm 1.6	29.4 \pm 1.5	30.6 \pm 1.4	N/A
TTA-A2 (n=16)	29.1 \pm 2.4	29.6 \pm 2.5	30.1 \pm 2.5	45.4 \pm 3.9
ML-218 (n=13)	31.3 \pm 2.7	31.8 \pm 2.7	32.3 \pm 2.7	54.1 \pm 4.2

Figure 1

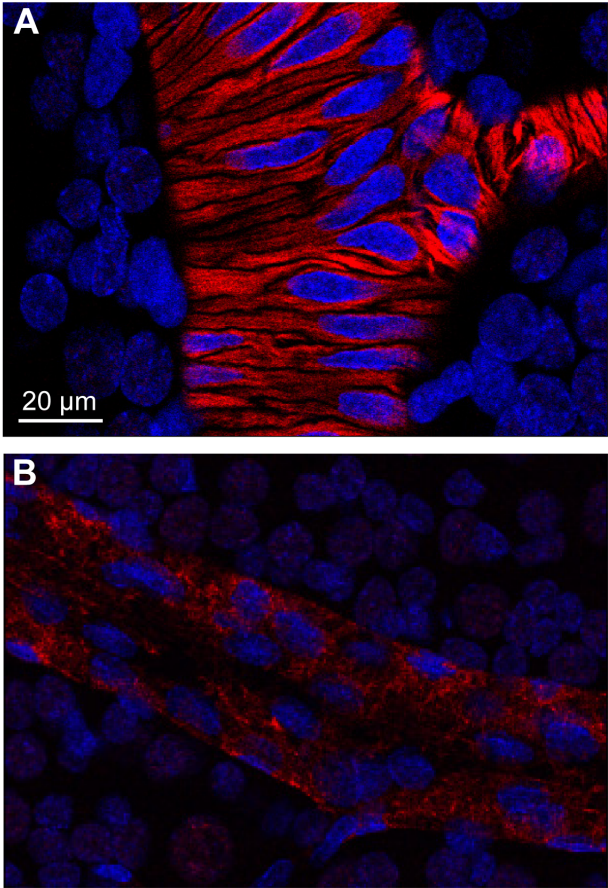


Figure 2

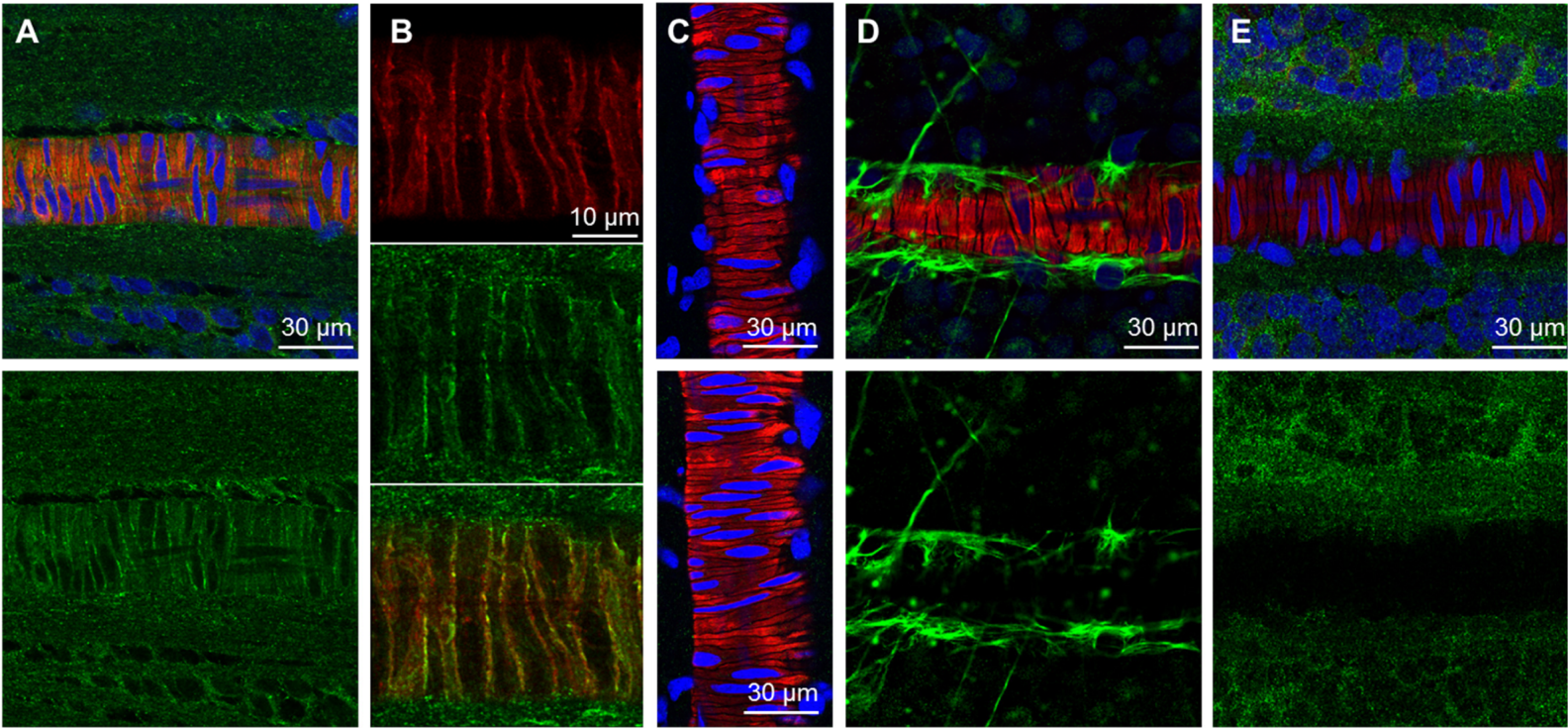


Figure 3

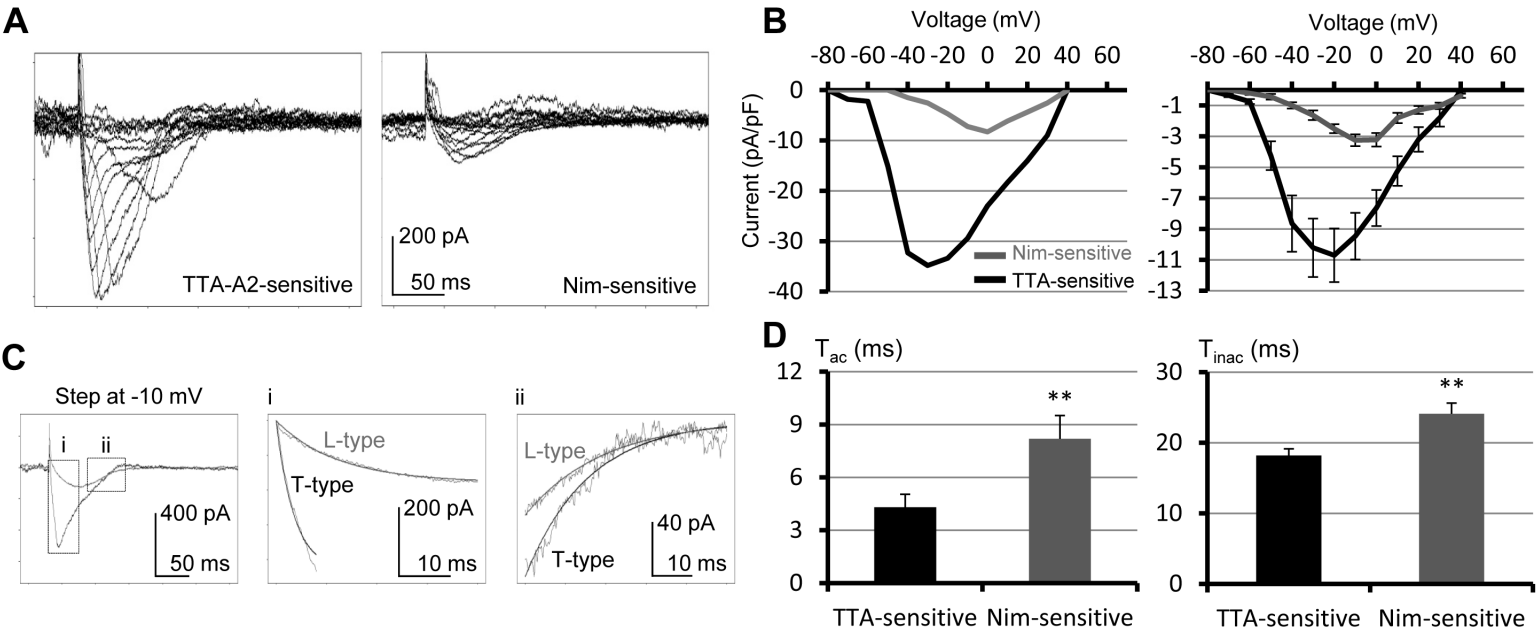


Figure 4

